

Selective Continuous Flow Iodination Guided by Direct Spectroscopic Observation of Equilibrating Aryl Lithium Regioisomers

Anna L. Dunn,^{*,†} David C. Leitch,^{*,†} Michel Journet,[†] Michael Martin,[‡] Elie A. Tabet,[‡] Neil R. Curtis,[§] Glynn Williams,[§] Charles Goss,^{||} Tony Shaw,[†] Bernie O'Hare,[⊥] Charles Wade,[§] Matthew A. Toczko,[‡] and Peng Liu[†]

[†]API Chemistry, GlaxoSmithKline, King of Prussia, Pennsylvania 19406, United States

[‡]Early Development Sciences, GlaxoSmithKline, Research Triangle Park, North Carolina 27709, United States

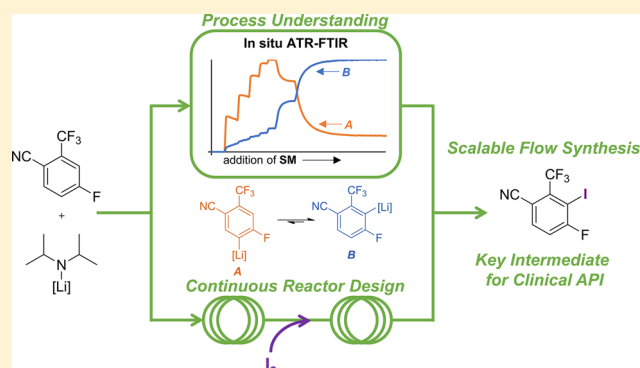
[§]API Chemistry, GlaxoSmithKline, Stevenage, U.K. SG1 2NY

^{||}Process Analytical Technologies, GlaxoSmithKline, King of Prussia, Pennsylvania 19406, United States

[⊥]Global Spectroscopy, GlaxoSmithKline, King of Prussia, Pennsylvania 19406, United States

Supporting Information

ABSTRACT: The iodination of 4-fluoro-2-(trifluoromethyl)benzonitrile via C–H lithiation and subsequent treatment with iodine under continuous flow conditions is described. Screening identified both LDA and PhLi as effective bases, giving the desired 3-iodo regioisomer as the major product. Use of LDA results in varying amounts of the undesired 5-iodo isomer, while PhLi results in more reliable formation of the 3-iodo product. An initial flow process was developed using PhLi that produced 4-fluoro-3-iodo-2-(trifluoromethyl)benzonitrile in 63% yield on a gram scale. Process modifications to enable pilot-scale operation resulted in a yield decrease to <50%, persistent formation of a byproduct resulting from PhLi addition to the nitrile, and formation of solids during longer runs. As a result, the use of LDA was investigated under continuous flow conditions. In situ NMR and IR spectroscopy allowed observation of the 5-[Li] species and its conversion to the thermodynamically preferred 3-[Li] species. These mechanistic insights drove development of a second-generation continuous flow process using LDA that achieves 30:1 regioselectivity and an 84% solution yield of the desired product (67% isolated yield after recrystallization). Furthermore, this process increases throughput by 10-fold, providing a path to manufacturing-scale operation.



INTRODUCTION

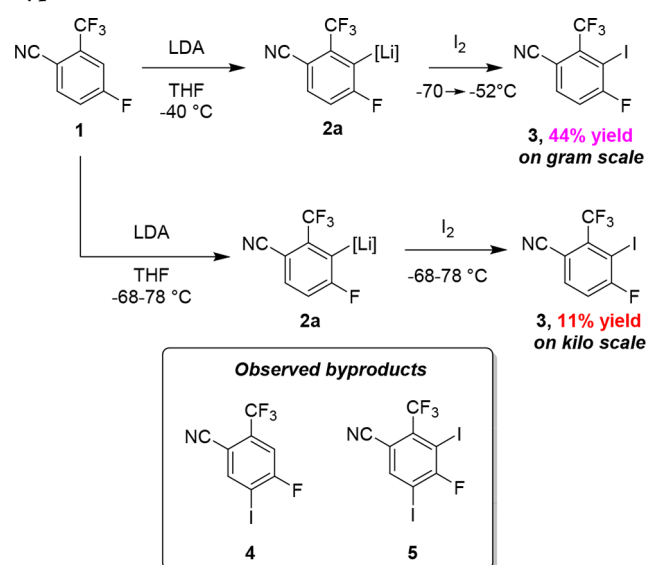
Halogenation of organometallic reagents is a powerful method to form C–X bonds in a highly regioselective manner.¹ This is particularly true for halogenation of electron-deficient aromatics, which will not readily undergo electrophilic aromatic substitution but are often excellent substrates for C–H metalation using strong bases such as lithium diisopropylamide (LDA).² As part of development efforts toward a selective androgen receptor modulator (SARM)³ clinical candidate, we required large amounts of the tetrasubstituted iodoarene **3** as an intermediate in the preparation of the active pharmaceutical ingredient (API) (Scheme 1). Prior work in our medicinal chemistry group focused on iodination of an ArLi species (**2a**) generated by regioselective metalation of 4-fluoro-2-(trifluoromethyl)benzonitrile (**1**) using LDA.⁴

While this chemistry was suitable to support discovery chemistry efforts, affording **3** in 44% isolated yield on a gram scale, attempts to scale up to kilogram quantities resulted in a precipitous reduction in yield (11%). This was due to decomposition and formation of multiple byproducts (**4**, **5**, and others not identified) despite considerable effort to modify the reaction conditions from those initially developed. Our hypothesis was that the ArLi species is unstable under the reaction conditions and therefore decomposed during the longer addition times and localized hot spots common to larger scale batch reactions,⁵ especially given the exothermicity of the

Special Issue: The Roles of Organometallic Chemistry in Pharmaceutical Research and Development

Received: July 30, 2018

Scheme 1. Initial Batch Synthesis of Iodoarene 3 with Byproducts 4 and 5



iodination step (~ 20 °C temperature rise observed in gram-scale runs).

Although alternative routes were evaluated, they all resulted in a significant increase in material costs, number of synthetic transformations, or both. Process chemistry efforts therefore focused on developing a reliable, large-scale method to prepare 3, requiring an in-depth study of this transformation to determine the cause of poor scalability. Herein we describe the development of a regioselective metalation/iodination that is amendable to multi-kilogram-scale preparation of 3, focusing on the use of continuous flow to alleviate mixing and energy transfer issues associated with the batch chemistry.⁶ Key to the success of the iodination is generation of the correct organometallic regioisomer (2a), which we have determined is the thermodynamically most stable ArLi species.⁷ By combining small-scale screening experiments with operando NMR and IR spectroscopy, we identified the key factors that lead to a selective and higher-yielding halogenation. These insights drove development of continuous processes using both PhLi and LDA as metalation reagents, enabling access to 3 in up to 67% isolated yield with a throughput of $425 \text{ g L}^{-1} \text{ h}^{-1}$.

RESULTS AND DISCUSSION

Batch Reaction Screening and Development. Given the scalability issues observed with the lithiation/iodination sequence described in Scheme 1, several other iodination approaches that would avoid the use of sensitive organometallic intermediates were investigated. Unfortunately, electrophilic iodination does not proceed using reagents such as ICl and NIS, undoubtedly due to the electron-deficient nature of 1.⁸ Catalytic C–H functionalization using Pd, Rh, or Ir systems under conditions described in the literature also failed to give the desired product.⁹ Rather than completely redesign the synthesis of the final API, we initiated a more thorough evaluation of metalation/iodination conditions to determine the causes for poor scalability.

A series of small-scale screening experiments was designed to evaluate the base, stoichiometry, temperature, and metalation time. Many bases other than LDA were evaluated, including PhLi, ⁿBuLi, the hexamethyldisilazide series (Li, Na,

K), KO^tBu, ⁱPrMgCl, and PhMgBr. With the exception of LDA and PhLi, these bases led to either no conversion of starting material or formation of new byproducts (tentatively identified as attack of the nitrile by nucleophilic bases such as ⁿBuLi).

Table 1 summarizes results obtained for LDA and PhLi with amounts of 1, 3, and 4 determined by HPLC assay or ¹⁹F

Table 1. Effect of Base Identity, Amounts, and Temperature on Yield and Regiochemistry of Iodination

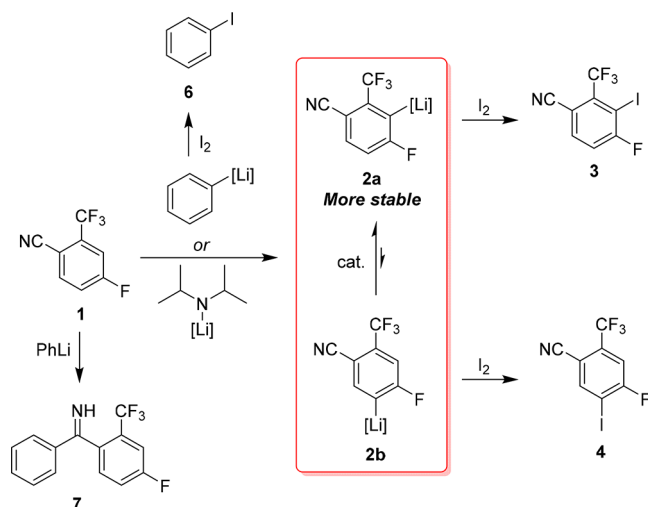
| entry | base ^a (equiv) | T (°C) | step 1 time (min) | 1 (%) ^b | 3 (%) ^b | 4 (%) ^b |
|-----------------|---------------------------|--------|-------------------|--------------------|--------------------|--------------------|
| 1 ^c | LDA (0.95) | -70 | 2 | 20 | 45 | 17 |
| 2 | LDA (1.05) | -45 | 0.33 | 13 | 56 | 20 |
| 3 | LDA (1.05) | -45 | 2 | 10 | 63 | 14 |
| 4 ^c | LDA (0.95) | -45 | 2 | 10 | 65 | 3 |
| 5 | LDA (1.05) | -45 | 5 | 10 | 75 | 4 |
| 6 | LDA (1.05) | -45 | 10 | 7 | 72 | 3 |
| 7 | LDA (1.05) | -30 | 0.33 | 12 | 63 | 2 |
| 8 | LDA (1.05) | -30 | 2 | 8 | 65 | 2 |
| 9 | LDA (1.05) | -30 | 5 | 11 | 48 | 2 |
| 10 | LDA (1.05) | -10 | 0.33 | 10 | 52 | 2 |
| 11 | PhLi (1.00) | -70 | 5 | 9 | 74 | 2 |
| 12 | PhLi (1.00) | -45 | 0.33 | 11 | 50 | 8 ^d |
| 13 ^c | PhLi (0.95) | -45 | 2 | 17 | 44 | 1 |
| 14 | PhLi (1.00) | -45 | 5 | 12 | 59 | 1 |
| 15 ^c | PhLi (1.00) | -30 | 0.33 | 7 | 28 | 2 |

^aAbbreviations: LDA, lithium diisopropylamide (prepared fresh from ⁿBuLi/HN(ⁱPr)₂ as a 1.0 M solution in THF/hexanes); PhLi, phenyllithium (commercial 1.8 M solution in ⁿBu₂O). Unless otherwise noted, the base was added in one portion to a solution of 1 (0.187 mmol). ^bSolution yield determined by HPLC assay. ^cBase added dropwise to a solution of 1 (0.800 mmol, 4 \times scale); solution yields determined by ¹⁹F NMR spectroscopy versus internal standard. ^dCoelution of 4 and PhI (6) resulted in an inflated assay yield of 4. ^eThe major product is imine 7 (Scheme 2).¹⁰

NMR spectroscopy versus internal standard. These data clearly show that metalation of 1 is rapid with either base, even at -70 °C. Using LDA, the amount of 4 generated is dependent on reaction time, temperature, and amount of base. At -70 °C, a 2 min deprotonation time gives 80% conversion of 1 and a $\sim 2.5:1$ ratio of 3 to 4 (entry 1). Increasing the temperature to -45 °C increases the conversion to $\sim 90\%$ even with only a 20 s metalation time; however, the ratio of 3 to 4 is still $<3:1$ (entry 2). Increasing the metalation time to 2 min improves the product ratio (entry 3), which is further improved by reducing the LDA charge (entry 4). The highest solution yield (75%) and best regioisomer ratio (19:1) is obtained with a 5 min metalation time at -45 °C (entry 5); increasing the reaction time to 10 min did not result in higher solution yield or improved regioisomer ratio (entry 6). At -30 °C, 20 s is sufficient to achieve a 63% solution yield of 3 (entry 7), with increased reaction times eventually leading to a drop in yield due to decomposition (entry 9). At -10 °C, 20 s is too long to prevent decomposition (entry 10), and attempts to metalate at 0 °C even at short reaction times led to complex mixtures with small quantities of 3 present.

Metalation/iodination with PhLi gave similar results, with two important distinctions. The levels of **4** observed are lower than with LDA (compare Table 1, entries 2 and 12), generally between only 1 and 2%, and there are two additional byproducts generated (Scheme 2). Iodobenzene (**6**) results

Scheme 2. Reaction Pathways for Lithiation/Iodination Using PhLi or LDA and Origin of Byproducts 4, 6, and 7^a



^aThermally sensitive intermediates are shown in the red box.

from iodination of unreacted PhLi, which can be mitigated by avoiding the use of excess base and ensuring a long enough reaction time to completely consume PhLi (compare entries 12 and 14). The primary imine **7** is formed through competitive attack of PhLi at the nitrile, analogous to decomposition observed with other nucleophilic bases (vide supra). This side pathway is more prevalent at elevated temperatures, contributing to lower solution yields at -45 and -30 °C in comparison with LDA (compare entries 5 and 14 and entries 7 and 15). In fact, with PhLi at -30 °C the major product is **7**.¹⁰

To account for the observations outlined in Table 1, we propose the reaction pathways in Scheme 2. Using LDA or PhLi to metalate **1** results in a mixture of equilibrating ArLi regioisomers **2a** and **2b**, where **2a** is thermodynamically preferred. This equilibration must be catalyzed by a proton source: equilibration of ArLi species using LDA has been

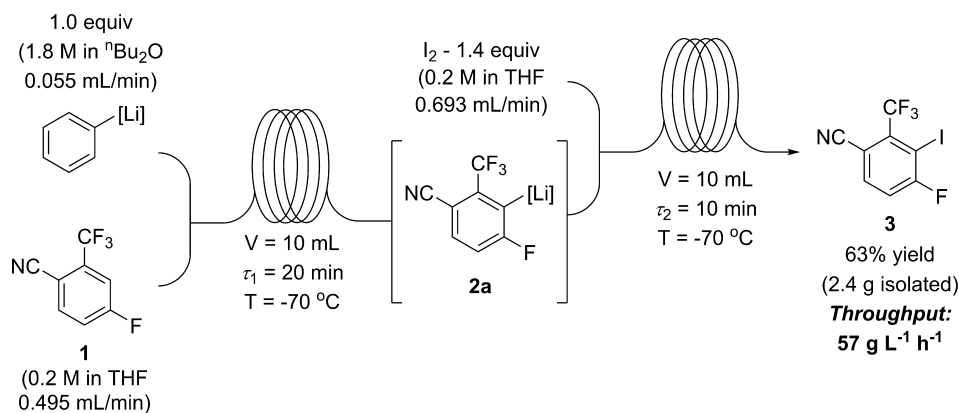
studied previously, indicating that diisopropylamine is a capable catalyst;^{2c–g} unreacted **1** could also initiate this interconversion by acting as a proton source. That **2a** is thermodynamically more stable is consistent with prior thermodynamic studies of the directing ability of fluorine and $-\text{CF}_3$ groups in multiply fluorinated aromatics conducted by Schlosser and co-workers.^{7b,c} For trifluorotoluene, the energy difference between the *o*- and *p*-lithium species is 2.7 kcal/mol at -75 °C in favor of the ortho regioisomer,^{7c} which matches well with the generally high regioselectivity observed (for example, Table 1, entry 11: $\sim 35:1$ ratio of **3** to **4** at -70 °C).

With LDA, shorter metalation reaction times and lower temperatures lead to an increase in the amount of **4**, leading us to suspect that **2b** may be the kinetically preferred metalation product using this base at -70 °C, likely due to a combination of sterics and lithium speciation (vide infra).^{2g} Unfortunately, the typical strategy of using higher reaction temperatures and longer times to ensure equilibration is not compatible with the observed thermal instability of these species. In contrast, using PhLi appears to directly generate a thermodynamic ratio of **2a**/**2b**; this could be through preferential metalation at the 3-position and/or rapid equilibration.^{2c–g}

Initial Continuous Process Development. From the data obtained in small-scale screening experiments, it is clear that careful control over short reaction times, maintenance of low temperatures during exothermic processes, and precise reaction stoichiometry are critical to ensuring the maximum yield of **3** regardless of whether LDA or PhLi is used. Regioisomer **4** is the most difficult contaminant to remove by crystallization; we therefore focused our development efforts on minimizing formation of this byproduct. Because the use of PhLi consistently leads to high regioselectivity, and the formation of **6** and **7** can be controlled with temperature and stoichiometry, initial process development efforts focused on these conditions.

Given the previous difficulties encountered in scaling this reaction, and the need to tightly control the reaction parameters and times, we eschewed batch chemistry development for a flow chemistry approach.⁶ The rapid reaction kinetics for both metalation and iodination are ideal for short residence time flow chemistry processes, and maintaining low reaction temperatures is much easier in smaller reactors with low reactive inventory, even for exothermic reactions. Many research groups in both academia and industry have taken advantage of flow chemistry for effecting difficult metalations,

Scheme 3. Schematic of Lab-Scale Flow Process for the Synthesis of 3 Using PhLi



including those that generate unstable intermediates that must be quenched quickly.^{11,12} The use of microreactors is one approach to this problem;^{6a,11c} however, our need for large-scale production is incompatible with the throughput afforded by microreactor systems.¹² Finally, one key challenge with organometallic chemistry in flow is the frequent generation of solids that lead to reactor clogging and overpressurization. While technologies exist to handle solid-containing streams, avoiding the formation of insoluble materials is preferable.

A laboratory-scale flow reactor was assembled according to Scheme 3. The feed lines and reactor loops (10 mL) were made of fluoropolymer tubing, all of which were submerged in a cold bath at $-70\text{ }^{\circ}\text{C}$. Standard syringe or HPLC pumps were used to deliver the reagent solutions, which were precooled in 1 mL loops before being mixed at simple T-junctions. A targeted set of conditions based on those from entry 11 in Table 1 were evaluated, maintaining the stoichiometry at 1.0 equiv of PhLi and 1.4 equiv of I_2 . In this reactor at $-70\text{ }^{\circ}\text{C}$, a 5 min residence time for deprotonation (τ_1) is not sufficient to reach >50% conversion of **1**. This apparently slower reactivity was attributed to improved heat transfer: even in small-scale batch experiments, the exothermic addition of PhLi could result in an increased internal reaction temperature, giving a faster apparent rate. Increasing τ_1 to 20 min by lowering the flow rates enables $\sim 90\%$ conversion of **1**, with >15:1 selectivity for the desired regioisomer **3**. Batch workup and isolation of a 150 mL fraction of flow output resulted in 63% yield after crystallization; this corresponds to a throughput (after purification) of $57\text{ g L}^{-1}\text{ h}^{-1}$.

After this gram-scale demonstration, the suitability of these conditions for multi-kilogram production of **3** was evaluated. Three major issues with the process outlined in Scheme 3 were identified: formation of the imine impurity **7**, leading to the need for low temperatures; the tendency of the reaction stream to generate solids during prolonged operation; and the low material throughput. Addressing this last point was critical: at $57\text{ g L}^{-1}\text{ h}^{-1}$, preparation of 10 kg of **3** using our $\sim 150\text{ mL}$ pilot-scale reactor¹⁰ would require almost 50 days of continuous processing time.

In order to increase the reaction rate, and operate within the temperature range of our pilot reactor, we raised the reaction temperature to $-50\text{ }^{\circ}\text{C}$. While this enables a reduction in total residence time to 5 min, the isolated yield of **3** under these conditions dropped to <50%. This is consistent with our small-scale screening experiments, where the solution assay of **3** drops 15% when the metalation temperature is increased from $-70\text{ }^{\circ}\text{C}$ to $-45\text{ }^{\circ}\text{C}$ (Table 1, compare entries 11 and 14); the drop in yield is due primarily to increased formation of **7**. We were able to supply 6.85 kg of **3** using this chemistry, but prolonged operation was not possible due to the formation of solids. One other practical concern manifested during our initial scale-up: THF solutions of iodine are not stable at ambient temperatures due to polymerization of the solvent.¹³ We were able to mitigate this issue by holding the iodine feed solution at $-16\text{ }^{\circ}\text{C}$ and using it within 3 days; however, use of an alternative solvent would be preferable. All of these factors drove us to develop a more robust process for long-term supply of **3**.

Revisiting LDA: Direct Observation of Equilibrating ArLi Isomers. Given that the formation of **7** is mostly responsible for the loss in yield, we re-evaluated the suitability of LDA for a continuous process. Understanding the factors that control the formation of putative ArLi regioisomers **2a** and

2b as a function of time, temperature, and reaction stoichiometry was therefore critical. To confirm our hypothesis that **2b** is the initial metalation product with LDA, which equilibrates to the thermodynamically preferred **2a**, we used low-temperature NMR spectroscopy to directly observe these species (Figure 1). Treatment of **1** with 0.95 equiv of LDA at

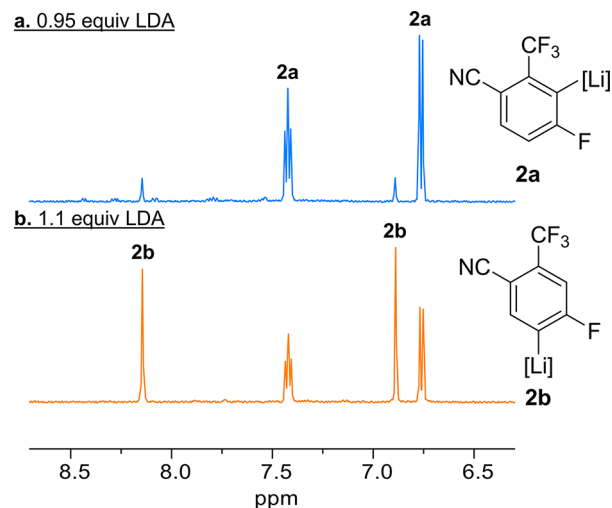


Figure 1. ^1H NMR spectra (500 MHz, $-70\text{ }^{\circ}\text{C}$, d_8 -THF) of **1** and (a) 0.95 or (b) 1.1 equiv of LDA. Poor selectivity in (b) is likely due to the sample warming above $-70\text{ }^{\circ}\text{C}$ during injection.

$-70\text{ }^{\circ}\text{C}$ results in one major species with spectral features consistent with **2a** (Figure 1a). In contrast, using a slight excess of LDA produces both **2a** and a second species consistent with **2b** in a 1.25:1 ratio; relative integration of the signals for **2a** and **2b** in the former case gives a $\sim 10:1$ ratio.¹⁴ Quenching these solutions with I_2 generates mixtures of **3** and **4** consistent with these assignments.¹⁰

While these NMR spectroscopic results support our hypothesis of thermodynamic control over regioselectivity in the metalation of **1**, we were unable to observe the initial metalation event or conversion between the two regioisomers due to rapid metalation occurring prior to spectral acquisition. An operando ATR-FTIR spectroscopic method capable of 10 s acquisition time allowed observation of the kinetics of the metalation and equilibration.¹⁵ An iterative metalation–quench protocol was employed to correlate IR spectral features to iodinated product distribution, revealing signals at 1105 and 1130 cm^{-1} that correspond to **2a** and **2b**, respectively. Figure 2 shows a representative reaction profile for the metalation of **1** conducted using an inverse addition (solution of **1** added dropwise to a solution of 0.95 equiv of LDA) at $-70\text{ }^{\circ}\text{C}$. The profile clearly shows rapid initial formation of **2b** followed by slower equilibration to **2a**. At $-70\text{ }^{\circ}\text{C}$ this equilibration takes approximately 20 min to reach steady state; at $-45\text{ }^{\circ}\text{C}$, both **2b** and **2a** are generated within 10 s, and complete equilibration to **2a** is complete in <90 s.¹⁰ The depletion of **2a** upon addition of I_2 is also extremely rapid and is complete essentially upon mixing, even at $-70\text{ }^{\circ}\text{C}$.

A titration experiment at $-70\text{ }^{\circ}\text{C}$ monitored by operando ATR-FTIR confirms that **2b** is the major regioisomer in the presence of excess LDA at low temperature, and equilibration occurs only once excess **1** is present (Figure 3). In fact, at the titration end point (Figure 3, point f), equilibration commences but stops prematurely. At low [**1**] and low

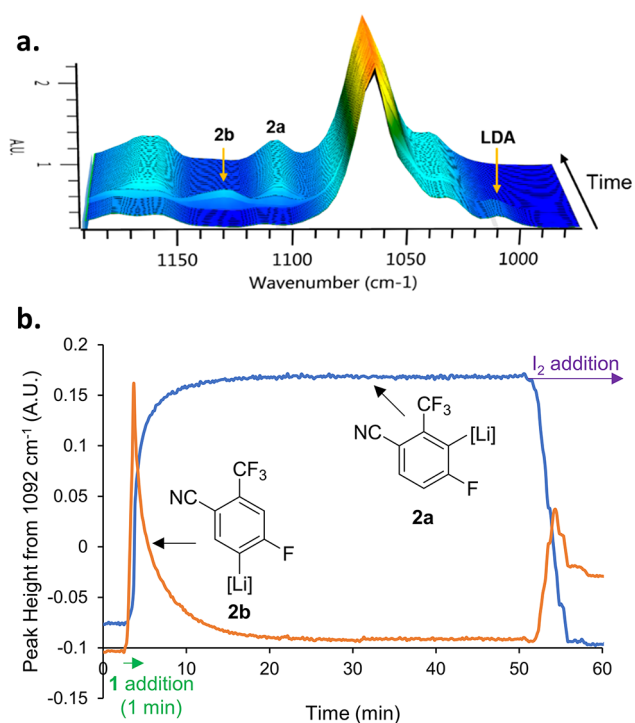


Figure 2. (a) Observation of the two aryllithium species under batch conditions via ATR-FTIR at $-70\text{ }^{\circ}\text{C}$ (**2a**, 1105 cm^{-1} ; **2b**, 1130 cm^{-1}). (b) Reaction progress plot. A THF solution of **1** was added over 1 min to a solution of LDA at the time indicated, and the I_2 solution was added dropwise at 50 min. Peak heights are relative to absorbance at 1092 cm^{-1} (single-point baseline).

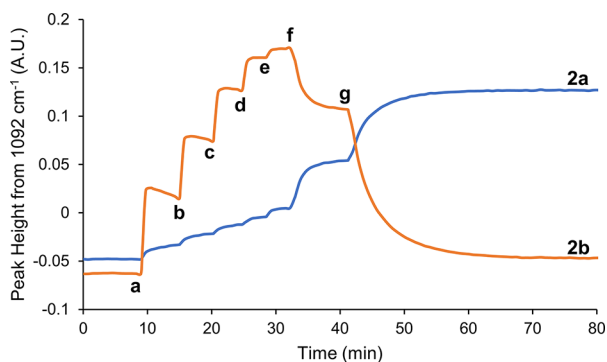


Figure 3. Titration of a THF solution of **1** into an LDA solution at $-70\text{ }^{\circ}\text{C}$ monitored by ATR-FTIR. At each point a–d, 0.21 equiv of **1** was added. At point e, 0.11 equiv of **1** was added, and 0.053 equiv of **1** was added at points f and g, totaling 1.06 equiv of **1** added. Note that at point f LDA and **1** are equimolar, leading to incomplete conversion to **2a**. Peak heights are relative to absorbance at 1092 cm^{-1} (single-point baseline).

[LDA], the rate of reaction between **1** and LDA is similar to the rate of equilibration, leaving unreacted **1** available to mediate the isomerization; as LDA finally consumes **1**, there is no longer an available proton source, and equilibration stops. These insights were used to set the stoichiometry (0.95 equiv of LDA) and residence time (4 min for metalation) for our subsequent flow experiments to ensure complete equilibration before quenching with iodine.

We then assessed the stability of **2a** at increasing temperatures (Figure 4). The ATR-FTIR signal for **2a** remains steady following formation at $-70\text{ }^{\circ}\text{C}$ and after warming to

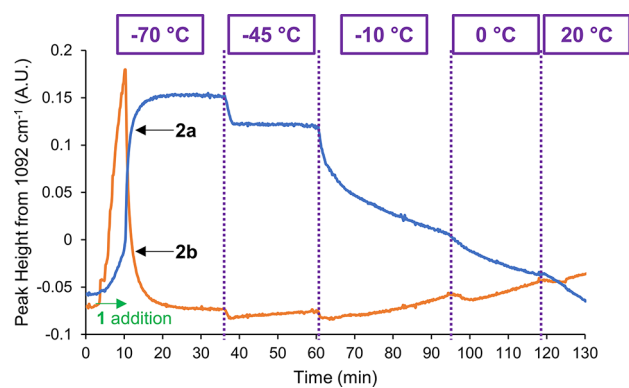


Figure 4. Stability of **2a** at a variety of temperatures as monitored by ATR-FTIR. A THF solution of **1** was added dropwise to a solution of LDA at the time indicated, followed by holding the solution at the specified temperature. Note that the initial decrease in **2a** signal upon warming to $-45\text{ }^{\circ}\text{C}$ is due to temperature-induced changes in absorbance intensity, and the apparent increase in **2b** at $-10\text{ }^{\circ}\text{C}$ is indicative of decomposition, not interconversion of isomers. Peak heights are relative to absorbance at 1092 cm^{-1} (single-point baseline).

$-45\text{ }^{\circ}\text{C}$ and holding for >20 min; a separate experiment indicates prolonged hold times at $-45\text{ }^{\circ}\text{C}$ do result in slow decomposition.¹⁰ Further warming to $-10\text{ }^{\circ}\text{C}$ caused multiple changes to the IR spectral features, including a large decrease in **2a** signal, reflecting instability. Thus, efficient heat transfer is critical to the success of this chemistry. On a small scale and in flow reactors, maintaining an internal temperature of $-45\text{ }^{\circ}\text{C}$ is readily achievable,^{6,11,12} whereas in large batch reactors, local temperature spikes would decompose **2a**.⁵ Furthermore, long addition times of both the base and iodine solutions would be required to control these highly exothermic reactions, which are not compatible with the thermal instability of **2a** over time, even at $-45\text{ }^{\circ}\text{C}$. The root cause of the poor yield shown in Scheme 1 is almost certainly the highly exothermic nature of the initial metalation and I_2 addition.

On the basis of the data for metalation with LDA, we redesigned our lab-scale flow system to incorporate smaller volume reactors for shorter residence times (Figure 5). All of the reactor tubing was composed of ethylene tetrafluoroethylene (ETFE, 1/16 in. outer diameter) for efficient heat transfer and chemical compatibility. Rather than using simple T-junctions, we incorporated in-line stainless steel active mixers (magnetically driven agitation in a tube, or MDAT) to ensure effective mixing, even at low flow rates.¹⁶ Each reagent line has a precooling loop prior to mixing, and the metalation residence time is more than long enough for equilibration to be complete, ensuring maximum [**2a**]. The reaction with I_2 occurs immediately upon mixing; therefore, we shortened the residence time to 16 s to increase throughput. The output stream is directly quenched into a stirred solution of aqueous sodium sulfite to destroy the excess I_2 ; failure to do so resulted in formation of poly-THF, which negatively affects product isolation.

The optimized flow process was performed with the following feed solutions: 0.33 M **1** in anhydrous THF (1 equiv), 0.31 M freshly prepared LDA in hexanes/anhydrous THF (0.95 equiv), and 0.49 M I_2 (1.5 equiv) in anhydrous 2-MeTHF with 10% toluene as an HPLC internal standard. This switch to 2-MeTHF alleviates the polymerization issue observed with THF: only trace polymer was observed by ^1H

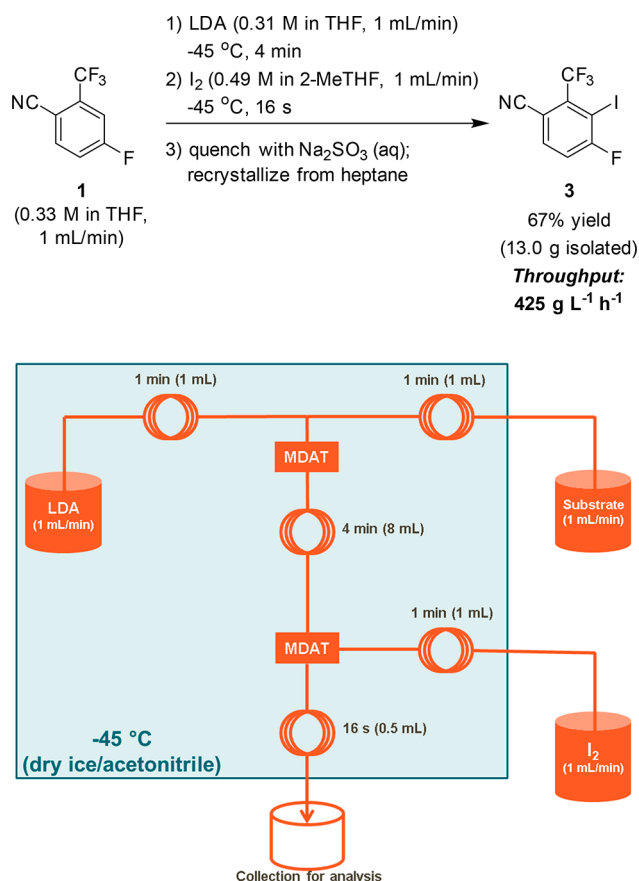


Figure 5. Multigram continuous flow run to produce **3** in 67% isolated yield using LDA and diagram of the lab-scale flow reactor. Everything within the box was placed in a dry ice/acetonitrile bath.

NMR spectroscopy after storing an I₂/2-MeTHF solution for 1 month.¹⁰ Attempts to use more concentrated feeds resulted in precipitation of solids, which we identified as a diisopropylammonium salt. Presumably this crystalline species is the product of diisopropylamine reacting with excess iodine prior to the quench to generate [iPr₂NH]⁺I⁻.¹⁷

Under the conditions shown in Figure 5, we were able to achieve an 84% solution yield of **3** over a >3 h run, with no solid formation or loss of purity over time. The iodination regioselectivity is 30:1 (determined by NMR spectroscopy), confirming complete ArLi equilibration within the 4 min residence time. Purification by crystallization from heptane gives **3** in 67% isolated yield, corresponding to a throughput (after purification) of 425 g h⁻¹ L⁻¹. This represents an improvement of almost 10-fold over the first-generation flow process described in Scheme 3, bringing the processing time needed to prepare 10 kg of **3** from >1 month to <1 week using our pilot-scale system. Work is currently underway to adapt this new process to pilot-scale production of this key intermediate for API synthesis.

CONCLUSIONS

By using a combination of small-scale screening experiments and mechanistic understanding gleaned through in situ spectroscopy, we have developed an efficient and selective lithiation/iodination sequence for the synthesis of a key pharmaceutical intermediate. The use of continuous flow chemistry is critical to the success of the C–H metalation,

which requires short reaction times, tight control over temperature and stoichiometry, and the intermediacy of unstable and interconverting organometallic species. The use of PhLi does give lower amounts of the regioisomeric impurity **4** under a wider range of conditions; however, direct attack of the phenyl anion at the nitrile leads to a significant amount of another byproduct (**7**), lowering the overall yield. In contrast, the use of LDA as the metalation reagent leads to the formation of two regioisomeric ArLi species. Direct observation of these ArLi intermediates, and the kinetics of their interconversion by operando IR spectroscopy, guided our efforts to develop the LDA-based sequence. This flow process has a throughput of 425 g L⁻¹ h⁻¹, which upon scale-up will meet our material production requirements. We have performed the chemistry on a multigram scale with 84% solution yield of the desired product and 67% isolated yield after recrystallization. As demonstrated by this work, the use of spectroscopy to observe reactive intermediates and study rapid kinetics is a powerful means for continuous flow process development and understanding.

EXPERIMENTAL SECTION

Materials. All common reagents, solvents, and compound **1** were purchased from commercial sources and used as received. Compounds **4**, **5**, and **7** were prepared and characterized as described in the Supporting Information.

NMR Spectroscopy. Ambient-temperature NMR spectra were acquired on a Bruker AVANCE III 400 MHz spectrometer (5 mm BBFO probe). Low-temperature NMR experiments were performed on a Bruker AVANCE III 500 MHz spectrometer (5 mm BBI probe). Chemical shifts were calibrated relative to residual protio solvent. Data were processed using TopSpin or MestreNova.

HPLC. Routine HPLC analysis was performed on Agilent 1100 or 1200 series instruments with diode array detectors. Unless otherwise noted, analysis was typically done with traces from a single wavelength with the following method: column, Zorbax SB-C18, 1.8 μm, 3 × 50 mm; column temperature, 60 °C; flow rate, 1.5 mL/min; solvent gradient, H₂O (0.05% TFA v/v)/ACN (0.05% TFA v/v), from 100/0 to 5/95 over 2.7 min; detection wavelength, 220 nm.

Table 1, entries 2, 3, 5–12, 14, and 15, used an Ascentis Express C18 column (100 mm × 4.6 mm; 2.7 μm): column temperature, 40 °C; flow rate, 1.5 mL/min; solvent gradient, H₂O (0.1% H₃PO₄)/ACN, from 70/30 to 0/100 over 2.5 min; detection wavelength, 228 nm for detection of **1**, **3**, and **4** and 210 nm for detection of **7**.

GC/MS. GC/MS analysis was performed on an Agilent 7890B GC/5977B MSD EI system using an HP-5MS column (30 m length, 0.25 mm diameter, 0.25 μm film): temperature ramp to 250 °C at a rate of 15 °C/min; hold time 10 min; run time 26 min.

Operando ATR-FTIR. Reactions were monitored by attenuated total internal reflection Fourier transform infrared spectroscopy (ATR-FTIR) using a Mettler Toledo ReactIR iC10 FTIR spectrometer with an MCT detector, HappGenzel apodization, and 1× gain. The diamond window ATR probe (DiComp, 9 mm diameter, 457 mm long, Hastelloy C22) was connected to the spectrometer by a 2 m silver halide optical fiber conduit. Prior to reaction monitoring, the background spectrum (256 scans) was obtained with the clean probe in air. Reaction spectra (2500–650 cm⁻¹, 8 cm⁻¹ resolution, 16 scans per spectrum) were collected at 10 s intervals using Mettler Toledo iCIR software v4.3.27.0 run on a Windows laptop computer. Reaction components were tracked using peak height profiles determined from reference spectra or assigned on the basis of analysis of changes in the reaction spectra.

SAFETY NOTE. Cryogenics can cause burns upon exposure. Wear proper PPE and avoid contact with cryogenics. Continuous flow equipment should be thoroughly leak-checked prior to operation, especially when reactive and potentially pyrophoric streams are used.

General Procedure for ATR-FTIR Experiments. Anhydrous THF (10 mL) and *N,N*-diisopropylamine (0.7 mL, 5.0 mmol, 0.95 equiv) were charged to a dried three-neck 100 mL round-bottom flask with a stir bar and ATR-FTIR probe under N_2 . The solution was cooled in a dry ice/acetone ($-70\text{ }^\circ\text{C}$) or dry ice/acetonitrile ($-45\text{ }^\circ\text{C}$) bath. $^n\text{BuLi}$ in hexanes (2.5 M, 2 mL, 5.0 mmol, 0.95 equiv) was added dropwise, followed by a solution of **1** (1.0 g, 5.3 mmol, 1 equiv) in 5 mL of anhydrous THF dropwise. At the indicated time, a solution of I_2 (2.0 g, 7.9 mmol, 1.5 equiv) was added dropwise.

General Procedure for Small-Scale Optimization Experiments. Table 1, Entries 1 and 4. Anhydrous THF (1 mL) was added to 150 mg of **1** (0.8 mmol, 1 equiv) in an 8 mL septum-capped vial with a stir bar under N_2 . In a separate 8 mL vial under N_2 in a dry ice/acetone or dry ice/acetonitrile cooling bath, an LDA solution was prepared with anhydrous THF (1 mL) and *N,N*-diisopropylamine (0.1 mL, 0.76 mmol, 0.95 equiv), followed by dropwise addition of 2.5 M $^n\text{BuLi}$ in hexanes (0.3 mL, 0.76 mmol, 0.95 equiv). The contents of both vials were stirred for 5 min in a dry ice/acetone bath for temperature equilibration. The LDA solution was added to the solution of **1** dropwise over 2 min via syringe to minimize the temperature rise from a reaction exotherm, followed by a solution of I_2 in 1 mL of anhydrous THF (303 mg, 1.19 mmol, 1.5 equiv) in one portion. The reaction was then quenched with 4 mL of saturated aqueous sodium sulfite (Na_2SO_3) solution, and 25 μL of 1,3,5-trifluorobenzene was added as a ^{19}F NMR internal standard. For NMR measurement, 100 μL of organic layer was added to 600 μL of CDCl_3 .

Table 1, Entry 13. As above, but PhLi (1.8 M in $n\text{Bu}_2\text{O}$, 444 μL , 0.800 mmol) was used instead of LDA.

Table 1, Entries 2, 3, and 5–10. *N,N*-Diisopropylamine (29.3 μL , 0.206 mmol) was dissolved in THF (90 μL) in a septum-cap-sealed 1.5 mL vial. The vial was cooled to $-5\text{ }^\circ\text{C}$ prior to the addition of $^n\text{BuLi}$ (2.5 M in hexanes, 79 μL , 0.197 mmol) over 5 s. In a separate vial containing a stirbar, **1** (35.4 mg, 0.187 mmol) was dissolved in THF (375 μL). The vial was sealed with a septum cap and cooled to $-70\text{ }^\circ\text{C}$ (dry ice/acetone) or $-45\text{ }^\circ\text{C}$ (dry ice/acetonitrile). A third vial was charged with I_2 (71.3 mg, 0.281 mmol) and THF (280 μL). The entire LDA solution was added via syringe in one portion to a stirred solution of **1**. This solution was stirred for the desired metalation time, followed by addition of the entire I_2 solution via syringe. The reaction was quenched 5 s later by the addition of 1 M HCl (1 mL). The entire reaction mixture was diluted to a total volume of 100 mL with MeOH and assayed by HPLC against calibrated absorbance values.

Table 1, Entries 11, 12, 14, and 15. As above, but PhLi (1.8 M in $^n\text{Bu}_2\text{O}$, 104 μL , 0.187 mmol) was used instead of LDA.

General Procedure for PhLi Lab-Scale Flow Reaction. Each line was primed with anhydrous THF at 1 mL/min for 20 min, and the reactor was submerged within a dry ice/acetone bath. Each feed solution was prepared as follows: (1) 7.57 g of **1** (40.0 mmol) was filled with anhydrous THF to a total final volume of 200 mL, (2) 15.2 g of I_2 (59.9 mmol) was filled with anhydrous THF to a total final volume of 300 mL, and (3) PhLi (1.8 M in $^n\text{Bu}_2\text{O}$, Sigma-Aldrich) was used as received. The stoichiometry of 1:PhLi:I_2 (1:1:1.4) was achieved by using flow rates of 0.495:0.055:0.693 mL/min. After reactor equilibration, 150 mL of product fractions was collected, combined with 50 mL of EtOAc, and washed with saturated aqueous Na_2SO_3 solution (50 mL) until complete discoloration was observed. The layers were separated, and the aqueous layer was washed with 20 mL of EtOAc. The combined organics were evaporated to dryness and added to 30 mL of heptane. The solution was heated to reflux to dissolve all solids and then cooled to ambient temperature. Solids were collected and rinsed with 5 mL of heptane, yielding 2.40 g of off-white product **3** (yield 64% based on 150 mL flow output theoretical yield).

Titration of **1 into LDA at $-70\text{ }^\circ\text{C}$ (Figure 3).** *N,N*-Diisopropylamine (0.71 mL, 5.0 mmol) and 5 mL of anhydrous THF were charged to a dry 50 mL three-necked round-bottom flask with stir bar and ATR-FTIR probe under N_2 . The solution was cooled to $-70\text{ }^\circ\text{C}$ in a dry ice/acetone bath, and $^n\text{BuLi}$ was added dropwise

(3.1 mL, 1.6 M in hexanes, 5.0 mmol). In an 8 mL vial, 1.0 g of **1** (5.2 mmol) was dissolved in 5 mL of anhydrous THF and flushed with N_2 . While IR spectra were acquired, a solution of **1** was added portionwise via syringe. A 1 mL portion of the **1** solution (1.05 mmol, 0.21 equiv) was added at 9, 15, 20, and 25 min. A 0.5 mL portion of the **1** solution (0.52 mmol, 0.11 equiv) was added at 29 min, and 0.25 mL (0.26 mmol, 0.053 equiv) was added at 33 and 41 min reaction time, totaling 1.06 equiv of **1** added.

General Procedure for LDA Lab-Scale Flow Reaction. All lines were primed with anhydrous THF (**1** and LDA lines) or 2-MeTHF (I_2 line) at 1 mL/min, and the reactor was submerged within a dry ice/acetonitrile bath ($-45.1\text{ }^\circ\text{C}$). The following feed solutions were prepared in 250 mL volumetric flasks: (1) 15.5 g of **1** (82 mmol, 1 equiv) filled with anhydrous THF and (2) 31.2 g of I_2 (123 mmol, 1.5 equiv) and 25 mL of toluene (internal standard) filled with 2-MeTHF. Each feed solution was added to feed bottles and placed under a positive pressure of N_2 . The LDA feed solution was prepared in the feed bottle with a stir bar: 208 mL of anhydrous THF and 10.9 mL of *N,N*-diisopropylamine (78 mmol, 0.95 equiv) were added under N_2 and cooled in a dry ice/acetonitrile bath, followed by dropwise addition of 31.1 mL of 2.5 M $^n\text{BuLi}$ in hexanes (78 mmol, 0.95 equiv). The LDA and **1** solutions, followed by the I_2 solution after 4 min, were pumped through the lines, each at a rate of 1 mL/min. After 10 min equilibration time, 5 min fractions were collected into 20 mL vials containing 6 mL of stirred saturated aqueous Na_2SO_3 to quench excess I_2 . After 50 min, 30 min fractions were collected into 175 mL bottles containing 50 mL of stirred saturated aqueous Na_2SO_3 . The fractions from 20 min to 3 h 33 min (input of 12.3 g of **1**) were combined into a 1 L separatory funnel with 200 mL of EtOAc and washed with 100 mL of saturated aqueous Na_2SO_3 combined with 50 mL of H_2O (2 \times), 0.5 M HCl (100 mL \times 3), and H_2O (1 \times 100 mL). The solvent was removed via rotary evaporation. ^1H NMR with 1,3,5-trimethoxybenzene added as an internal standard indicated a purity of 78%, giving an NMR yield of 84% of **3**. In a 500 mL round-bottom flask, the product was added to 160 mL of heptane and heated in a water bath to $70\text{ }^\circ\text{C}$ until all solids dissolved. The flask was slowly cooled to room temperature and then was cooled in an ice bath. The resulting solids were collected by filtration and rinsed with 80 mL of cold heptane to provide 13.0 g of **3** as an off-white solid (67% isolated yield).

■ ASSOCIATED CONTENT

Supporting Information

The Supporting Information is available free of charge on the ACS Publications website at DOI: 10.1021/acs.organomet.8b00538.

Flow reactor information, further information on NMR and ATR-FTIR experiments, characterization data, and 2-MeTHF polymerization data (PDF)

■ AUTHOR INFORMATION

Corresponding Authors

*E-mail for A.L.D.: anna.l.dunn@gsk.com.

*E-mail for D.C.L.: david.c.leitch@gsk.com; dcleitch@uvic.ca.

ORCID

Anna L. Dunn: 0000-0003-2852-7755

David C. Leitch: 0000-0002-8726-3318

Notes

The authors declare no competing financial interest.

■ ACKNOWLEDGMENTS

The authors thank all of the members of the global Continuous Primary group, Pilot Plant Operations, and former colleagues at Research Triangle Park for their assistance during the course of this work.

REFERENCES

- (1) Larock, R. C.; Zhang, L. Halogenation of Organometallics. In *Comprehensive Organic Transformations: A Guide to Functional Group Preparations*, 3rd ed.; Larock, R. C., Ed.; Wiley: Hoboken, NJ, 2018; pp 1467–1480.
- (2) (a) Gschwend, H. W.; Rodriguez, H. R. Heteroatom-Facilitated Lithiations. *Org. React.* **1979**, *26*, 1–360. (b) Snieckus, V. Directed Ortho Metalation. Tertiary Amide and O-Carbamate Directors in Synthetic Strategies for Polysubstituted Aromatics. *Chem. Rev.* **1990**, *90*, 879–933. (c) Cottet, F.; Schlosser, M. Three Chloro-(trifluoromethyl)pyridines as Model Substrates for Regioexhaustive Functionalization. *Eur. J. Org. Chem.* **2004**, *2004*, 3793–3798. (d) Collum, D. B.; McNeil, A. J.; Ramirez, A. Lithium Diisopropylamide: Solution Kinetics and Implications for Organic Synthesis. *Angew. Chem., Int. Ed.* **2007**, *46*, 3002–3017. (e) Viciu, M. S.; Gupta, L.; Collum, D. B. Mechanism of Lithium Diisopropylamide-Mediated Substitution of 2,6-Difluoropyridine. *J. Am. Chem. Soc.* **2010**, *132*, 6361–6365. (f) Fukuda, T.; Ohta, T.; Sudo, E.; Iwao, M. Directed Lithiation of N-Benzenesulfonyl-3-bromopyrrole. Electrophile-Controlled Regioselective Functionalization via Dynamic Equilibrium between C-2 and C-5 Lithio Species. *Org. Lett.* **2010**, *12*, 2734–2737. (g) Hoepker, A. C.; Gupta, L.; Ma, Y.; Faggin, M. F.; Collum, D. B. Regioselective Lithium Diisopropylamide-Mediated Ortholithiation of 1-Chloro-3-(trifluoromethyl)benzene: Role of Autocatalysis, Lithium Chloride Catalysis, and Reversibility. *J. Am. Chem. Soc.* **2011**, *133*, 7135–7151. (h) Florio, S.; Salomone, A. Heterocycle-Mediated ortho-Functionalization of Aromatic Compounds: The DoM Methodology and Synthetic Utility. *Synthesis* **2016**, *48*, 1993–2008.
- (3) Mohler, M. L.; Bohl, C. E.; Jones, A.; Coss, C. C.; Narayanan, R.; He, Y.; Jin Hwang, D.; Dalton, J. T.; Miller, D. D. Nonsteroidal Selective Androgen Receptor Modulators (SARMs): Dissociating the Anabolic and Androgenic Activities of the Androgen Receptor for Therapeutic Benefit. *J. Med. Chem.* **2009**, *52*, 3597–3617.
- (4) Turnbull, P. S.; Cadilla, R. Indolecarbonitriles as Selective Androgen Receptor Modulators. PCT Int. Appl. WO 2014013309A1/20140123, 2014.
- (5) (a) McConville, F. X. *The Pilot Plant Real Book: A Unique Handbook for the Chemical Process Industry*; FXM Engineering and Design: Worcester, MA, 2002. (b) Stoessel, F. *Thermal Safety of Chemical Processes: Risk Assessment and Process Design*; Wiley-VCH: Weinheim, Germany, 2008. (c) Davis, E. M.; Viswanath, S. K. Heat Transfer Based Scale-Down of Chemical Reactions. *Org. Process Res. Dev.* **2012**, *16*, 1360–1370.
- (6) (a) Yoshida, J.; Takahashi, Y.; Nagaki, A. Flash chemistry: flow chemistry that cannot be done in batch. *Chem. Commun.* **2013**, *49*, 9896–9904. (b) Gutmann, B.; Cantillo, D.; Kappe, C. O. Continuous-Flow Technology—A Tool for the Safe Manufacturing of Active Pharmaceutical Ingredients. *Angew. Chem., Int. Ed.* **2015**, *54*, 6688–6729. (c) Baumann, M.; Baxendale, I. R. The Synthesis of Active Pharmaceutical Ingredients (APIs) using Continuous Flow Chemistry. *Beilstein J. Org. Chem.* **2015**, *11*, 1194–1219. (d) Porta, R.; Benaglia, M.; Puglisi, A. Flow Chemistry: Recent Developments in the Synthesis of Pharmaceutical Products. *Org. Process Res. Dev.* **2016**, *20*, 2–25. (e) Movsisyan, M.; Delbeke, E. I. P.; Berton, J. K. E. T.; Battilocchio, C.; Ley, S. V.; Stevens, C. V. Taming Hazardous Chemistry by Continuous Flow Technology. *Chem. Soc. Rev.* **2016**, *45*, 4892–4928. (f) May, S. A. Flow Chemistry, Continuous Processing, and Continuous Manufacturing: A Pharmaceutical Perspective. *J. Flow Chem.* **2017**, *7*, 137–145. (g) Plutschack, M. B.; Pieber, B.; Gilmore, K.; Seeberger, P. H. The Hitchhiker's Guide to Flow Chemistry. *Chem. Rev.* **2017**, *117*, 11796–11893.
- (7) (a) Schlosser, M. The 2 × 3 Toolbox of Organometallic Methods for Regiochemically Exhaustive Functionalization. *Angew. Chem., Int. Ed.* **2005**, *44*, 376–393. (b) Hyla-Kryspin, I.; Grimme, S.; Büker, H. H.; Nibbering, N. M. M.; Cottet, F.; Schlosser, M. The Gas Phase Acidity of Oligofluorobenzenes and Oligochlorobenzenes: About the Additivity or Non-Additivity of Substituent Effects. *Chem. - Eur. J.* **2005**, *11*, 1251–1256. (c) Gorecka-Kobylinska, J.; Schlosser, M. Relative Basicities of ortho-, meta-, and para-Substituted Aryllithiums. *J. Org. Chem.* **2009**, *74*, 222–229.
- (8) (a) Merkushev, E. B. Advances in the Synthesis of Iodoaromatic Compounds. *Synthesis* **1988**, *1988*, 923–937. (b) Rozen, S.; Zamir, D. A Novel Aromatic Iodination Method Using F₂. *J. Org. Chem.* **1990**, *55*, 3552–3555.
- (9) (a) Kalyani, D.; Dick, A. R.; Anani, W. Q.; Sanford, M. S. A Simple Catalytic Method for the Regioselective Halogenation of Arenes. *Org. Lett.* **2006**, *8*, 2523–2526. (b) Mei, T.-S.; Giri, R.; Mangel, N.; Yu, J.-Q. Pd^{II}-Catalyzed Monoselective ortho Halogenation of C-H Bonds Assisted by Counter Cations: A Complementary Method to Directed ortho Lithiation. *Angew. Chem., Int. Ed.* **2008**, *47*, 5215–5219. (c) Schroder, N.; Wencel-Delord, J.; Glorius, F. High-Yielding, Versatile, and Practical [Rh(III)Cp*]-Catalyzed Ortho Bromination and Iodination of Arenes. *J. Am. Chem. Soc.* **2012**, *134*, 8298–8301. (d) Partridge, B. M.; Hartwig, J. F. Sterically Controlled Iodination of Arenes via Iridium-Catalyzed C-H Borylation. *Org. Lett.* **2013**, *15*, 140–143.
- (10) See the [Supporting Information](#) for more details.
- (11) (a) Kupracz, L.; Kirschning, A. Multiple Organolithium Generation in the Continuous Flow Synthesis of Amitriptyline. *Adv. Synth. Catal.* **2013**, *355*, 3375–3380. (b) Pieber, B.; Glasnov, T.; Kappe, C. O. Flash Carboxylation: Fast Lithiation – Carboxylation Sequence at Room Temperature in Continuous Flow. *RSC Adv.* **2014**, *4*, 13430–13433. (c) Westermann, T.; Mleczko, L. Heat Management in Microreactors for Fast Exothermic Organic Syntheses – First Design Principles. *Org. Process Res. Dev.* **2016**, *20*, 487–494.
- (12) (a) Newby, J. A.; Blaylock, D. W.; Witt, P. M.; Turner, R. M.; Heider, P. L.; Harji, B. H.; Browne, D. L.; Ley, S. V. Reconfiguration of a Continuous Flow Platform for Extended Operation: Application to a Cryogenic Fluorine-Directed ortho-Lithiation Reaction. *Org. Process Res. Dev.* **2014**, *18*, 1221–1228. (b) Kopach, M. E.; Cole, K. P.; Pollock, P. M.; Johnson, M. D.; Braden, T. M.; Webster, L. P.; McClary Groh, J.; McFarland, A. D.; Schafer, J. P.; Adler, J. J.; Rosemeyer, M. Flow Grignard and Lithiation: Screening Tools and Development of Continuous Processes for a Benzyl Alcohol Starting Material. *Org. Process Res. Dev.* **2016**, *20*, 1581–1592. (c) Thaisrivongs, D. A.; Naber, J. R.; McMullen, J. P. Using Flow to Outpace Fast Proton Transfer in an Organometallic Reaction for the Manufacture of Verubecstat (MK-8931). *Org. Process Res. Dev.* **2016**, *20*, 1997–2004. (d) Laue, S.; Haverkamp, V.; Mleczko, L. Experience with Scale-Up of Low-Temperature Organometallic Reactions in Continuous Flow. *Org. Process Res. Dev.* **2016**, *20*, 480–486. (e) Feng, R.; Ramchandani, S.; Ramalingam, B.; Wei Benjamin Tan, S.; Li, C.; Khean Teoh, S.; Boodhoo, K.; Sharratt, P. Intensification of Continuous Ortho-Lithiation at Ambient Conditions – Process Understanding and Assessment of Sustainability Benefits. *Org. Process Res. Dev.* **2017**, *21*, 1259–1271. (f) Usutani, H.; Cork, D. G. Effective Utilization of Flow Chemistry: Use of Unstable Intermediates, Inhibition of Side Reactions, and Scale-Up for Boronic Acid Synthesis. *Org. Process Res. Dev.* **2018**, *22*, 741–746.
- (13) Cataldo, F. Iodine: A Ring Opening Polymerization Catalyst for Tetrahydrofuran. *Eur. Polym. J.* **1996**, *32*, 1297–1302.
- (14) The ¹H NMR signals assigned to **2b** appear as singlets, whereas coupling to F should be observed (as it is for **2a**). We attribute this apparent lack of coupling to a rapid monomer/dimer equilibrium for **2b** at –70 °C, analogous to that observed for PhLi. For **2a**, steric hindrance likely prevents dimerization, enabling observation of coupling. For solution dynamics of PhLi, see: Reich, H. J.; Green, D. P.; Medina, M. A.; Goldenberg, W. S.; Gudmundsson, B. O.; Dykstra, R. R.; Phillips, N. H. Aggregation and Reactivity of Phenyllithium Solutions. *J. Am. Chem. Soc.* **1998**, *120*, 7201–7210.
- (15) (a) Li, X.; Leonori, D.; Sheikh, N. S.; Coldham, I. Synthesis of 1-Substituted Tetrahydroisoquinolines by Lithiation and Electrophilic Quenching Guided by In Situ IR and NMR Spectroscopy and Application to the Synthesis of Salsolidine, Carnegine and Laudanosine. *Chem. - Eur. J.* **2013**, *19*, 7724–7730. (b) Keles, H.; Susanne, F.; Livingstone, H.; Hunter, S.; Wade, C.; Bourdon, R.; Rutter, A. Development of a Robust and Reusable Microreactor

Employing Laser Based Mid-IR Chemical Imaging for the Automated Quantification of Reaction Kinetics. *Org. Process Res. Dev.* **2017**, *21*, 1761–1768. (c) Li, H.; Sheeran, J. W.; Clausen, A. M.; Fang, Y.-Q.; Bio, M. M.; Bader, S. Flow Asymmetric Propargylation: Development of Continuous Processes for the Preparation of a Chiral β -Amino Alcohol. *Angew. Chem., Int. Ed.* **2017**, *56*, 9425–9429. (d) Carter, N.; Li, X.; Reavey, L.; Meijer, A. J. H. M.; Coldham, I. Synthesis and Kinetic Resolution of Substituted Tetrahydroquinolines by Lithiation then Electrophilic Quench. *Chem. Sci.* **2018**, *9*, 1352–1357.

(16) Dolman, S. J.; Nyrop, J. L.; Kuethe, J. T. Magnetically Driven Agitation in a Tube Mixer Affords Clog-Resistant Fast Mixing Independent of Linear Velocity. *J. Org. Chem.* **2011**, *76*, 993–996.

(17) Southwick, P. L.; Christman, D. R. Reactions of Unsaturated Compounds with Iodine-Amine Complexes. I. Reactions of Benzalacetophenone and Benzalacetone. *J. Am. Chem. Soc.* **1952**, *74*, 1886–1891.